Malaysian Journal of Science **21**: 85-92 (2002)

Differential cross sections for e^+-H scattering at intermediate energies

M. Z. M. Kamali, K. K. Rajagopal and **Kuru Ratnavelu**

Institute of Mathematical Sciences, University of Malaya, 50603 Kuala Lumpur, Malaysia

ABSTRACT The coupled-channel optical method (CCOM) has been used to study positron scattering by atomic hydrogen. Nine-state (H(1s), H(2s), H(2p), H(3s), H(3p), H(3d), Ps(1s), Ps(2s), Ps(2p)) and six-state basis set (H(1s), H(2s), H(2p), Ps(1s), Ps(2s), Ps(2p)) and the continuum optical potential has been used in our calculations. We present our results for the differential cross section (DCS) for the 1s-1s, 1s-2s and 1s-2p transitions at 50, 100 and 200 eV.

ABSTRAK Kaedah 'coupled-channel optical method' (CCOM) telah digunakan bagi mengkaji kesan perlanggaran suatu zarah positron ke atas atom hidrogen. Suatu ruang asas yang besar : sembilan asas (H(1s), H(2s), H(2p), H(3s), H(3p), H(3d), Ps(1s), Ps(2s), Ps(2p)) dan enam asas (H(1s), H(2s), H(2p), Ps(1s), Ps(2s), Ps(2p)) bersama-sama dengan 'continuum optical potential' telah diimplementasikan dalam penyelidikan ini. Dengan ini keputusan – keputusan bagi 'differential cross section (DCS)' diperlihatkan bagi transisi-transisi 1s-1s, 1s-2s dan 1s-2p pada 50, 100 dan 200 eV.

(continuum optical potential, positronium (Ps), differential cross section (DCS))

INTRODUCTION

In the last 10-12 years, we have seen major developments in the theoretical as well as experimental studies on the positron-hydrogen atom scattering system [1]-[17]. Most of the theoretical calculations have reported various cross sections such as ionization cross section (ICS), total cross section (TCS) and total positronium formation cross section (TPsfCS) for this scattering system.

In particular, the theoretical works of Kernoghan *et.al* [3] and Mitroy [9] are regarded as the benchmark for these cross sections as their calculations show reasonable qualitative as well as quantitative agreement with experimental measurements [4], [6], [15], [16]. Nevertheless, there are some quantitative differences between their calculations for a number of these cross sections. They have also not reported any differential cross sections (DCS) for positron-hydrogen atom scattering. In view of the differences seen between these calculations, it would also be useful to compare the DCS for these transitions. The DCS should provide a more discriminating test between theories.

The present work extends the work of Ratnavelu and Rajagopal [10] by implementing the coupled-channel optical method (CCOM) with improved numerical techniques [13], [14] and we report the differential cross section for major transitions on e^+-H scattering. We are not able to compare our DCS with the works of Kernoghan *et. al* [3] or Mitroy [9] due to the lack of DCS data from their calculations. So, we compare our present DCS with the work of Walters [7]. Walters has used the multi-pseudostate close-coupling (MPCC) calculation to perform the most comprehensive study of positron-hydrogen scattering at intermediate energies ranging from 54.4 – 300 eV. His MPCC method is a single-centre close-coupling calculation and has neglected the Ps channels in its expansion. Thus, our present work should provide a useful comparative study of the neglect of Ps channels at intermediate energies.

THEORY

The details of the CCOM can be found in Rajagopal and Ratnavelu [11]. Here, we will briefly outline the main aspects of the CCOM. The momentum space Lippmann-Schwinger equations for a positron with momentum $\mathbf{k}$ incident on hydrogen atom in state ψ_α (atomic units are assumed throughout) are

$$\langle \mathbf{k}'\phi_{\beta'}|T|\mathbf{k}\psi_\alpha\rangle = \langle \mathbf{k}'\phi_{\beta'}|V|\mathbf{k}\psi_\alpha\rangle + \sum_{\alpha''}\int d^3k'' \frac{\langle \mathbf{k}'\phi_{\beta'}|V|\mathbf{k}''\phi_{\alpha''}\rangle\langle \mathbf{k}''\psi_{\alpha''}|T|\mathbf{k}\psi_\alpha\rangle}{\left(E^{(+)} - \varepsilon_{\alpha''} - \frac{1}{2}k''^2\right)}$$

$$+ \sum_{\beta''}\int d^3k'' \frac{\langle \mathbf{k}'\phi_{\beta'}|V|\mathbf{k}''\phi_{\beta''}\rangle\langle \mathbf{k}''\phi_{\beta''}|T|\mathbf{k}\psi_\alpha\rangle}{\left(E^{(+)} - \varepsilon_{\beta''} - \frac{1}{4}k''^2\right)} \qquad (1)$$

and

$$\langle \mathbf{k}'\psi_{\alpha'}|T|\mathbf{k}\psi_\alpha\rangle = \langle \mathbf{k}'\psi_{\alpha'}|V^{(Q)}|\mathbf{k}\psi_\alpha\rangle + \sum_{\alpha''}\int d^3k'' \frac{\langle \mathbf{k}'\psi_{\alpha'}|V^{(Q)}|\mathbf{k}''\psi_{\alpha''}\rangle\langle \mathbf{k}''\psi_{\alpha''}|T|\mathbf{k}\psi_\alpha\rangle}{\left(E^{(+)} - \varepsilon_{\alpha''} - \frac{1}{2}k''^2\right)}$$

$$+ \sum_{\beta''}\int d^3k'' \frac{\langle \mathbf{k}'\psi_{\alpha'}|V|\mathbf{k}''\phi_{\beta''}\rangle\langle \mathbf{k}''\phi_{\beta''}|T|\mathbf{k}\psi_\alpha\rangle}{\left(E^{(+)} - \varepsilon_{\beta''} - \frac{1}{4}k''^2\right)} \qquad (2)$$

The generic term V is used to label the interaction between different classes of channels and the details can be found in Mitroy and Ratnavelu [8].

Using the Feshbach [17] formalism, we define the projection operators P and Q as follows

$$P = \sum_{\alpha\in P}|\psi_\alpha\rangle\langle\psi_\alpha| \qquad (3)$$

$$Q = 1 - P$$

$$P^2 = P,\ Q^2 = Q$$

$$PQ = QP = 0 \qquad (4)$$

With these above definitions, it can be shown that

$$P\left(E - K - v_2 - V^{(Q)}\right)P\Psi_n = 0 \qquad (5)$$

where eq. (5) is an approximation to the original Schrodinger equation. The optical potential $V^{(Q)}$ consists of a first-order static-exchange potential and a non-local complex polarization term. The real and imaginary parts of the complex polarization potential describe virtual and real excitations of the Q-space channels, respectively. Set Q includes the target continuum channels and the remainder of the discrete channels that are not explicitly coupled in the coupled-channels calculation. In the present work, we are attempting to incorporate the local polarization potential into a coupled-channels calculation for positron-hydrogen scattering. The details of the optical potential $V^{(Q)}$ and its computation can be found in Rajagopal and Ratnavelu [10].

RESULTS AND DISCUSSIONS

The following calculations were performed:

(i) CC(3,3): This close-coupling calculation includes the hydrogen states H(1s), H(2s), H(2p) together with the positronium states Ps(1s), Ps(2s) and Ps(2p).
(ii) CCO(3,3): In this calculation, the six states in (i) are used together with the continuum optical potentials in the 1s-1s, 1s-2s, 1s-2p, 2s-2s, 2s-2p and 2p-2p couplings.
(iii) CC(6,3): Here the n=1, 2 and 3 (1s, 2s, 2p, 3s, 3p and 3d) hydrogen states are included in the expansion together with three physical Ps(1s, 2s and 2p) states.
(iv) CCO(6,3): The continuum optical potentials for the 1s-1s, 1s-2s, 1s-2p, 2s-2s, 2s-2p and 2p-2p are included within the CC(6,3) calculation.

Our calculations were done at the energy regime of 50 – 200 eV. In general, we allowed the Ps matrix elements for angular momentum $J \leq 22$, and the Lippmann-Schwinger (LS), equations (1) and (2), were solved. For $23 \leq J \leq 50$, the LS equations were solved without the Ps matrix elements. In the CCO(m,n) calculations, the continuum optical potentials were allowed for $0 \leq J \leq 24$ at $E \leq 50$ eV and $0 \leq J \leq 45$ at $E >$ 50 eV. In all the calculations here, we have used modifications suggested by Ratnavelu *et. al* [12] to perform the Gaussian integrations with a five-panel composite mesh. A quadrature mesh of 68 points was used for all the calculations.

i) Elastic scattering differential cross section

We depict the elastic DCS at 50, 100 and 200 eV in Fig. 1(a), (b) and (c) respectively. Our present calculations CCO(6,3) and CCO(3,3) are compared with the multi-pseudostate close-coupling (MPCC) calculations of Walters [7]. From Figs. 1(a)-(c), we observe a dip in the DCS for forward scattering predicted by the CC(6,3) and CC(3,3) model. This unusual feature vanishes with the inclusion of the optical potentials (CCO(6,3) and CCO(3,3)). The CC(6,3) and CC(3,3) calculations are also closer to the MPCC calculation as both energy and scattering angle increases.

In Fig. 1(a), both the CC(6,3) and CC(3,3) calculations predict larger cross section at the middle scattering angles between 15^0 to 100^0 than other theoretical datas. These differences become smaller and closer to the MPCC as the angle increases. The effect of the continuum in the CCO(6,3) and CCO(3,3) calculations reduces the DCS by about 7 - 43% when compared to the CC(m,n) calculations at $15^0 - 80^0$. Above 80^0, the inclusion of the optical potential enhances the DCS quite significantly. The differences between our present (CCO(6,3) and CCO(3,3)) and MPCC calculations can be seen obviously at forward and backward scattering angles. The CCO(6,3) and CCO(3,3) calculations overestimate the MPCC calculation for $\theta > 60^0$. Good agreement between the CCO(m,n) and the MPCC calculations at 45^0 - 60^0 is observed.

In Fig. 1(b), we show the elastic DCS at 100 eV. We find that, the CCO(6,3) and CCO(3,3) agrees quite well with the MPCC calculations. Some minor differences can still be seen in the forward scattering angle between the CCO(m,n) and the MPCC calculations. The effect of the continuum in the CCO(6,3) and CCO(3,3) calculations help to reduce the DCS significantly through out most of the angles presented here when compared to the corresponding CC(m,n) calculations. Convergence between the CCO(6,3) and CCO(3,3) is achieved as the scattering angles become larger.

The elastic DCS for 200 eV is depicted in Fig. 1(c). As expected, the resemblance between our CCO(6,3) and CCO(3,3) models with the MPCC is quite similar. The differences between the CC(6,3) and CC(3,3) models with the MPCC are smaller. As expected at higher energies, the contribution of the Ps channels become insignificant. A slight shoulder is still seen in the smaller scattering angles ($15^0 - 20^0$) predicted by the CCO(6,3) and CCO(3,3) models.

Generally, in the elastic case, the contribution of the rearrangement channels does play an important role in the calculation particularly at lower energies. The inclusion of the Ps channels, enhance or reduce the cross sections. This can be gauged by comparing the TPsfCS with the cross section given in Table 1. At 50 eV, the CCO(6,3) and CCO(3,3) calculations show that, the TPsfCS contributes about 24 - 26% of the TCS, which have been ignored by the MPCC calculations. At 100 and 200 eV, the contribution of the TPsFCS is about 3 - 4% and 0.2 – 0.3% respectively of the TCS. Thus, the effects of Ps formation should be less at this energy. This is evident in comparing the DCS between MPCC and CCO calculations.

ii) 1s-2s differential cross section

The DCS for 1s-2s excitation are illustrated in Figs. 2(a), (b) and (c) for 50, 100 and 200 eV respectively.

In Fig. 2(a), we show the DCS for H(1s-2s) transition at 50 eV. Both the present calculations (CCO(6,3) and CCO(3,3)) show only slight differences with the MPCC models. The CCO(m,n) enhances the cross section by about 10 – 52% for the scattering angles between 30^0 – 60^0, in comparison to the corresponding CC(m,n) calculations. This is due to the contribution of the continuum effects in the calculations. We also observe that the CCO is closer to the MPCC data at this scattering angles. The CCO calculations also predict larger cross sections at the backward scattering angles compared to other theoretical works.

The DCS for H(1s-2s) transition at 100 eV is depicted, in Fig. 2(b). Generally, at 100 eV, all theories show similar qualitative trends except for the CCO(6,3) and CCO(3,3) models, where there is a slight shoulder at about 15^0 –20^0. The existence of this slight shoulder may be due to the continuum effects in the calculation and not because of the Ps channels. In fact, both the CC(6,3) and CC(3,3) calculations seems to be in good agreement with the MPCC calculation except for $\theta \geq 70^0$. As the angle increases, the effect of the continuum in the CCO calculations seem to enhance the cross section.

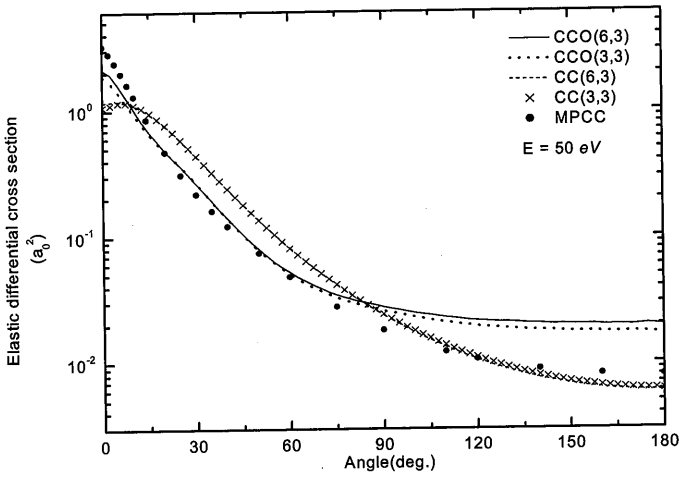

Figure 1(a): Elastic differential cross section (a_0^2) at 50eV

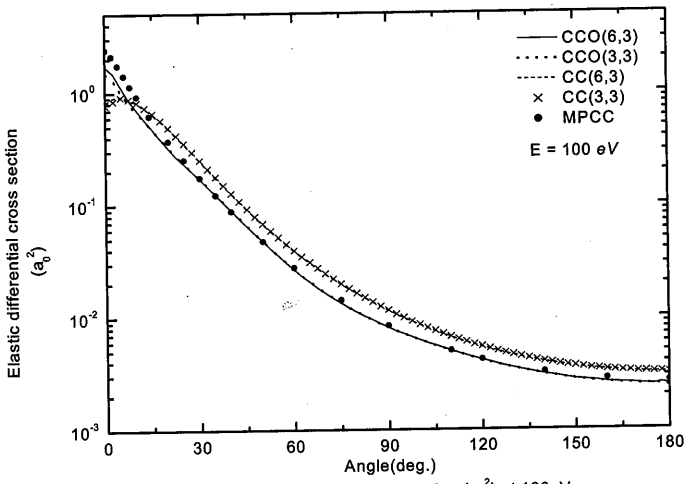

Figure 1(b): Elastic differential cross section (a_0^2) at 100eV

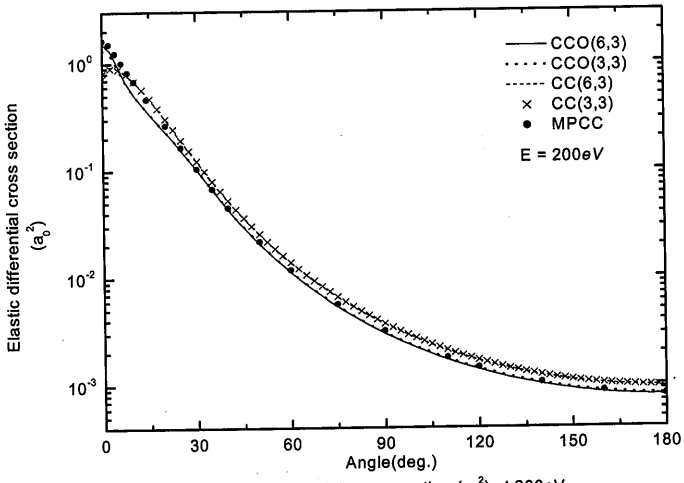

Figure 1(c): Elastic differential cross section (a_0^2) at 200eV

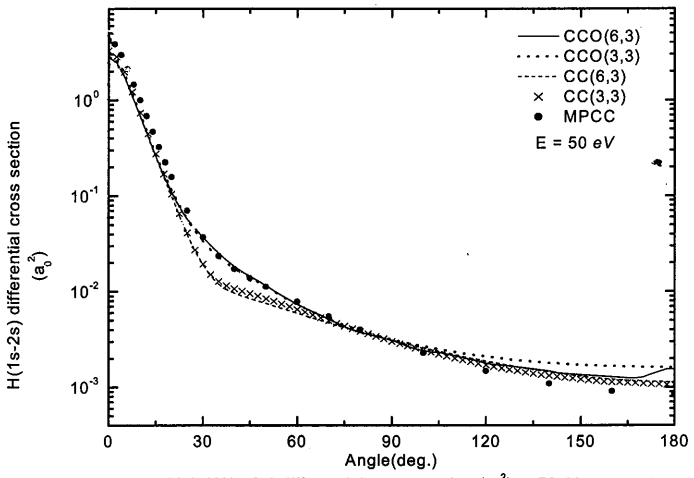

Figure 2(a): H(1s-2s) differential cross section (a_0^2) at 50eV

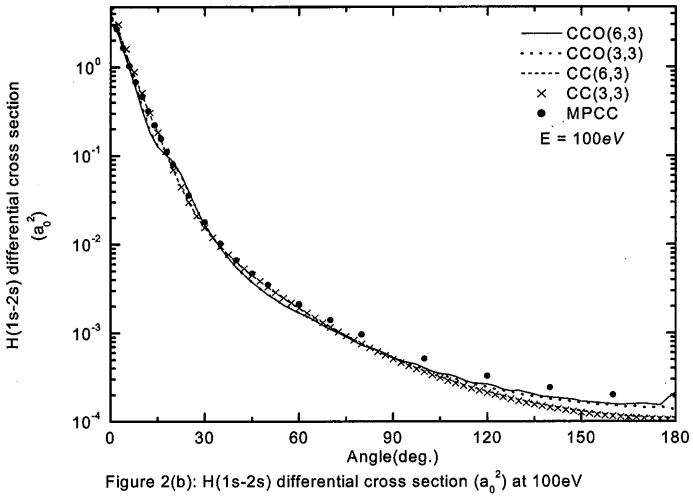

Figure 2(b): H(1s-2s) differential cross section (a_0^2) at 100eV

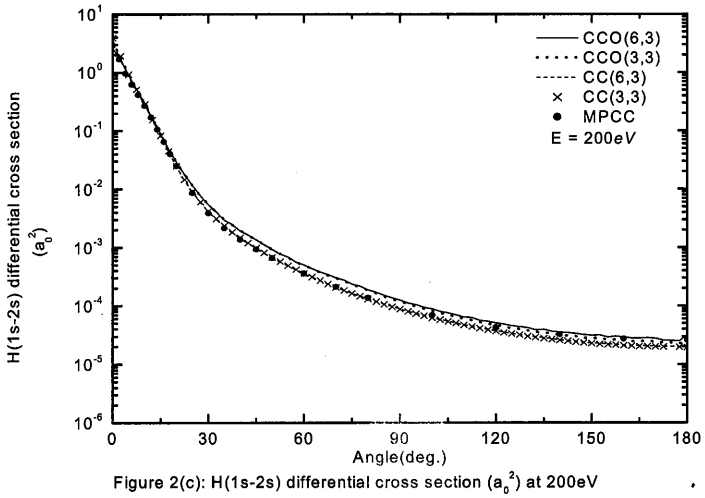

Figure 2(c): H(1s-2s) differential cross section (a_0^2) at 200eV

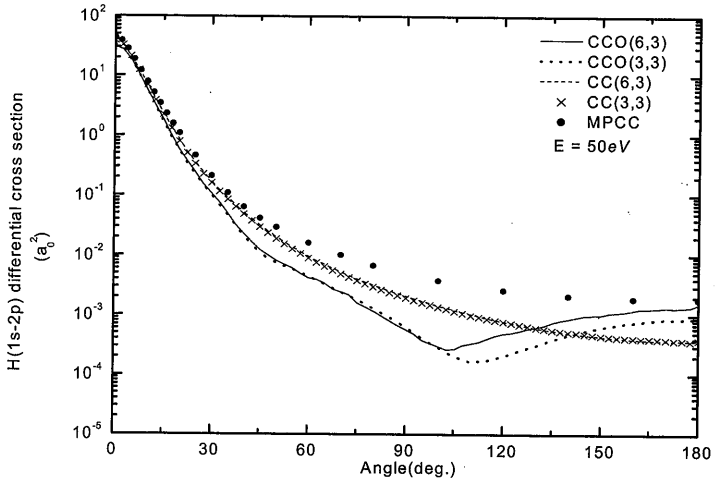

Figure 3(a): H(1s-2p) differential cross section (a_0^2) at 50eV

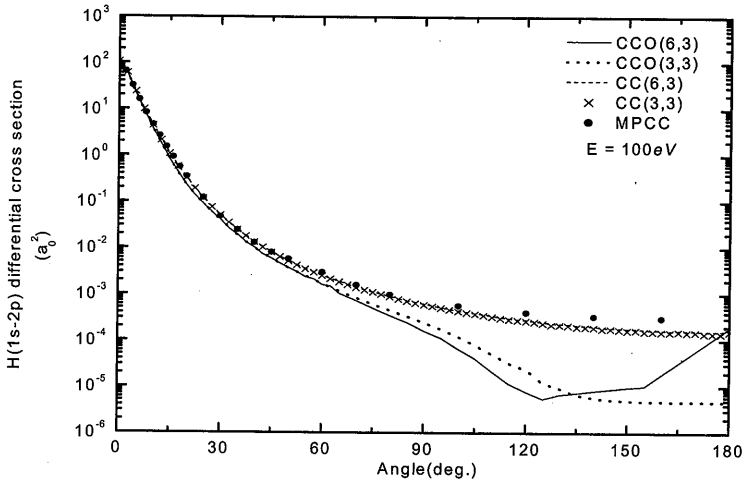

Figure 3(b): H(1s-2p) differential cross section (a_0^2) at 100eV

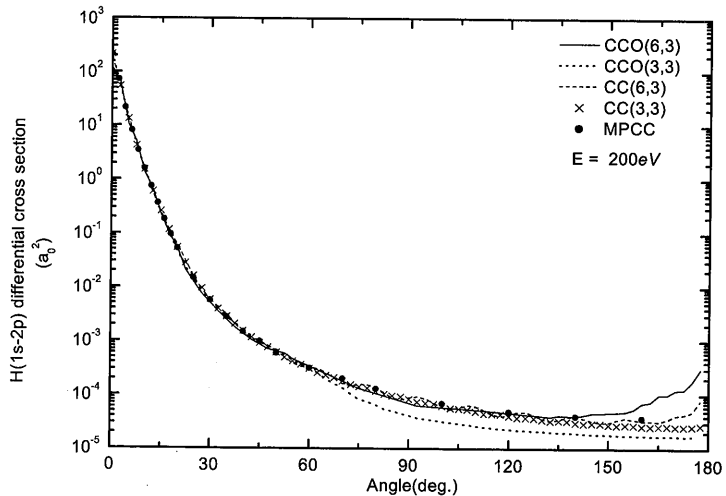

Figure 3(c): H(1s-2p) differential cross section (a_0^2) at 200eV

Table 1. Total cross sections for various transitions in units of πa_0^2

eV	50	100	200
Elastic Cross Section			
CCO(6,3)	0.3204	0.1807	0.1109
CCO(3,3)	0.3065	0.1792	0.1105
CC(6,3)	0.4117	0.2402	0.1352
CC(3,3)	0.4136	0.2431	0.1357
MPCC	0.297	0.205	0.127
Total Cross Section			
CCO(6,3)	2.8634	1.9273	1.2269
CO(3,3)	2.6971	1.7955	1.1378
CC(6,3)	2.2301	1.2463	0.728
CC(3,3)	2.0711	1.107	0.6548
MPCC	3.02	2.24	1.33
Total Ps formation Cross Section			
CCO(6,3)	0.6995	0.0651	0.0036
CCO(3,3)	0.7115	0.0671	0.0037
CC(6,3)	0.8518	0.0715	0.0039
CC(3,3)	0.8724	0.0737	0.004

The DCS for H(1s-2s) transition at 200 eV is shown in Fig. 2(c). The present calculations (CCO(6,3), CCO(3,3), CC(6,3) and CC(3,3)) show quite good agreement with the MPCC model. The differences between the present models and the MPCC calculations are very minor. The inclusion of Ps channels does not contribute very much in the present calculations (CCO(6,3), CCO(3,3), CC(6,3) and CC(3,3)) especially at the higher energies. This is shown by the close resemblance between the present work and the MPCC calculation. This, obviously shows that the Ps channels are only significant at low energies such as 50 eV.

iii) 1s-2p differential cross section

The DCS for H(1s-2p) transition at 50 eV is shown in Fig. 3(a), both the CCO models predict a slight shoulder at about 40^0-50^0 and broad minima at about 105^0 – 120^0 region. The CC and the MPCC models do not show this qualitative shape. The CCO(6,3) and CCO(3,3) calculations show large differences by reducing the cross section very significantly at $\theta > 50^0$ when compared to the MPCC. These differences become smaller as the scattering angle increases.

In Fig. 3(b) and Fig. 3(c), the DCS for the H(1s-2p) transition at 100 and 200 eV, is shown respectively. Both the CCO models give good agreement with the MPCC calculation at smaller scattering angles. At 100 eV, as the scattering angles become larger, both the CCO models predict smaller cross sections than those of the MPCC data. However, at 200 eV, only the CCO(6,3) predict larger cross section at backward angles. The broad minima at 100 eV, predicted by the CCO(6,3) model at around 120^0-150^0, vanishes at 200 eV.

In the H(1s-2p) transition case, we find that, the effect of the rearrangement channels are less significant in the present calculations. The CCO and CC calculations show general qualitative shapes which is similar to the MPCC model with some minor quantitative differences. For the CC(m,n) calculations, these differences are due to the Ps channels and become closer to the MPCC as the energy increases. The broad minima in the CCO(6,3) and CCO(3,3) which appear at 50 and 100 eV is believed to be caused by the inclusion of the optical potentials. Overall, the effect of the Ps channels is very significant at 50 eV (as compared to the MPCC). The continuum effects are also significant even at 100 eV.

CONCLUSION

The inclusion of the rearrangement channels, have played an important role in our present calculations (CCO(6,3), CCO(3,3), CC(6,3) and CC(3,3)). Walters has completely ignored the Ps channels in his calculation using the MPCC model. Thus, the validity of the MPCC calculation is limited. The effect of the Ps channels can be seen especially at lower intermediate energies such as 50 eV. Although, our present work have similar qualitative features with the MPCC model, there are some quantitative differences between them. As we increase the incident energy, these differences become smaller and our results tend to be closer to the MPCC calculation. Overall, the inclusion of Ps channels is very important in describing the physics of positron-scattering by atoms.

Acknowledgements K.R. would like to acknowledge the Malaysian Ministry of Science, Technology and Environment under the IRPA Project No. 09-02-03-1009 for funding of this project. MZMK thanks the MOSTE for the research assistantship under this grant.

REFERENCES

1. Kernoghan, A.A., McAlinden, M.T. and Walters, H.R.J. (1994). *J. Phys. B: At. Mol. Opt. Phys.* **27**: L211-L215
2. Kernoghan, A.A., McAlinden, M.T. and Walters, H.R.J. (1995). *J. Phys. B: At. Mol. Opt. Phys.* **28**: 1079-1094
3. Kernoghan, A.A., Robinson, D.J.R., McAlinden, M.T. and Walters, H.R.J. (1996). *J. Phys. B* **29**: 2089-2102
4. Hoffmann, A., Falke, T., Raith, W., Weber, M., Becker, D.P. and Lynn, K.G. (1997). *J. Phys. B: At. Mol. Opt. Phys.* **30**: 3297-3303
5. Bransden, B.H., McCarthy, I.E. and Stelbovics, A.T. (1985). *J. Phys. B: At. Mol. Opt. Phys.* **18**: 823-827
6. Jones, G.O., Charlton, M., Slevin, J., Laricchia, G., Köver, A., Poulsen, M.R. and Chormaic, S.N. (1993). *J. Phys. B: At. Mol. Opt. Phys.* **26**: L483-L488
7. Walters, H.R.J. (1988). *J. Phys. B: At. Mol. Opt. Phys.* **21**: 1893-1906
8. Mitroy, J. and Ratnavelu, K. (1995). *J. Phys. B: At. Mol. Opt. Phys.* **28**: 287-306
9. Mitroy, J. (1996). *Aust. J. Phys.* **49**: 919-936
10. Ratnavelu, K. and Rajagopal, K.K. (1999). *J. Phys. B* **32**: L381-L387
11. Rajagopal, K.K. and Ratnavelu, K. (2000). *Phys. Rev. A* **62**: 022717-9
12. Ratnavelu, K., Mitroy, J. and Stelbovics, A.T. (1996). *J. Phys. B* **29**: 2775-2796
13. Kamali, M.Z.M. (2002). *A Coupled-Channels Optical Study of Positron Scattering by Atomic Hydrogen.* MSc. thesis (unpublished).
14. Kamali, M.Z.M. and Ratnavelu, K. (2002). *Phys. Rev. A* **65**: 014702- 4
15. Weber, M., Hofmann, A., Raith, W., Sperber, W., Jacobsen, F.M. and Lynn, K.G. (1994). *Hyperfine Interact.* **89**: 221-242
16. Zhou, S., Li, H., Kauppilla, W.E., Kwan, C.K. and Stein, T.S. (1997). *Phys. Rev. A* **55**: 361-368
17. Feshbach, H. (1962) *Ann. Phys.* **19**: 287-313